


Effects of the γ -irradiation strength and basalt additive content on the mechanical performance and dielectric response of polypropylene films

Mehmet Kılıç ¹, Zeynep Güven Özdemir,¹ Ümit Alkan,² Yaşar Karabul,¹ Orhan İçelli¹

¹Department of Physics, Yıldız Technical University, 34220, Istanbul, Turkey

²Department of Computer Engineering, Istanbul Gelişim University, 34215, Istanbul, Turkey

Correspondence to: M. Kılıç (E-mail: kilic-m@hotmail.com)

ABSTRACT: In this study, we investigated the effects of high-dose γ -ray irradiation on the mechanical and dielectric properties of polypropylene (PP)-basalt thick films. PP-basalt thick-film composites with various basalt contents from 0.5 to 10.0% were prepared by a hot-press method. The samples were exposed to γ radiation at different doses in the range 3–25 kGy. The mechanical properties of the samples, such as the Young's modulus, tensile strength, percentage strain at break, and energy at break, were examined in the context of the γ -irradiation process. Although the maximum elasticity was obtained for the unirradiated 0.5% basalt-added composite, the 6 kGy γ -irradiated PP-1.0% basalt sample exhibited the highest elasticity properties among all of the composites. The best mechanical properties, including the ultimate tensile strength and energy at break values, were achieved for the 12 kGy γ -irradiated neat PP. The dielectric properties of the PP-basalt composites were also investigated in the 100 Hz to 15 MHz frequency region at room temperature. According to the analysis of the dielectric properties, the 3 kGy γ -irradiated neat PP may have potential for microelectronic device applications that require low dielectric constant and dielectric loss materials. © 2019 Wiley Periodicals, Inc. *J. Appl. Polym. Sci.* **2019**, *136*, 47414.

KEYWORDS: Composites; Dielectric properties; Differential Scanning Calorimetry (DSC); Mechanical Properties; Thermoplastics

Received 14 July 2018; accepted 18 November 2018

DOI: 10.1002/app.47414

INTRODUCTION

In recent years, there have been numerous studies focused on the effects of low- and high-dose γ radiation on materials that result in a noticeable outcome. The γ -irradiation method is also commonly applied technique for the modification of the mechanical, physical, and chemical attributes of commercial polymers.¹ A large number of studies have been reported on the effects of γ -ray exposure on polymer physical properties and chemical structures.² In particular, the mechanical and electrical properties of polymers can be modified with the γ -ray irradiation procedure. Recent studies have revealed that although a low-dose radiation application improves the mechanical properties of polymers, a high-dose radiation makes their mechanical parameters, such as their tensile strength and energy at break, worse.^{3–5} Additionally, Nouh *et al.*⁶ showed that a decrease in the conductivity of the makrofol polymer occurred because of the irradiation process. The effects of irradiation on the electrical conductivity have been described by the fact that crosslinking lessened the crystallinity and induced further lattice disorders, which could behave as energy barriers and scattering centers for the flow of electric current. For γ -irradiated copolymer films, the reduction of the direct-current (dc) conductivity was noticed by Fawzy *et al.*,⁷ and

this effect was interpreted as an occurrence of probable crosslinking in the copolymer films. Moreover, it was suggested that the decrease in dc conductivity was due to the formation of some defects in the energy gap as a result of γ irradiation. Along with the decrease in the dc conductivity, Raghu *et al.*⁸ reported that the dielectric permittivity increased with increasing irradiation dose for polymers. They explained changes in the dielectric response of the polymer in the form of the breaking of bonds, bending, discontinuity, crosslinking, chain scission, and so on in the molecular chains due to irradiation by the presence of an appreciable number of defects. Generally, the irradiation of polymers causes main-chain scission, crosslinking, and the evolution of hydrogen. These reactions strongly depend on the physical and chemical conditions of the polymer and the characteristics of the irradiation.² Various polymers have different responses to radiation, which are intrinsically associated with their chemical structures.

Polymers with low and high dielectric constants can be used for different technological purposes. Polymers with controllable dielectric properties have become very important in recent years. The dielectric properties of polymers having values not in the desired level can either be altered by the irradiation process or

use an inorganic additive. It has been known for a long time that the dielectric properties of polymers are adversely affected by exposure to nuclear radiation. The investigation of the change in the dielectric properties is of importance because of the widespread use of dielectrics in nuclear environments and the continuous increase in the amount of radiation that electrical equipment is supposed to withstand. Among other polymers, polypropylene (PP), which has widespread use in many biomedical products, degrades very easily with irradiation and suffers perhaps more than any other thermoplastic material. Resistant additives to the polymer, such as basalt and metal oxides, can eliminate this effect. A great deal of scientific research has also been done to ensure that PP and its composites are suitable radiation-shielding materials.^{9,10} In this respect, a low-cost and high-performance engineering polymer, PP, was chosen as a host matrix for improving its mechanical and dielectric properties via an electromagnetic irradiation process. The influence of electron-beam and γ -ray irradiation of commercial PP films' dielectric, mechanical and thermal properties were studied by Pawde and Parab¹¹ and Abiona and Osinkolu,³ respectively. Keene *et al.*¹² also studied the physical and mechanical properties of γ -irradiated PP nonwoven textiles with different doses of radiation up to 25 kGy. They determined that the Fourier transform infrared (FTIR) spectra of the irradiated samples indicated an increase in carbonyl groups. They also showed that the physical and mechanical properties of PP became worse with 25 kGy of γ irradiation. On the other hand, Khan *et al.*¹³ improved the mechanical properties of PP sheets by irradiating them with a γ -radiation dose of 500 krad.

Because PP, which is a clear glossy film with a high strength, has a moderate barrier to moisture, gases, and odors,¹⁴ PP with improved mechanical and thermal properties has crucial importance for the food packaging industry. On the other hand, as mentioned before, some polymer capacitors based on semicrystalline thermoplastics, such as PP, have attracted a great deal of attention because of their desirable properties, such as their light weight, low cost, and excellent processability for forming thin films with large surface areas. From this point of view, researchers have attempted to improve the dielectric, mechanical, and thermal properties of commercial PP films for various industrial applications, such as energy storage and packaging, through both γ -irradiation processes and the use of basalt filler. The main reasons for the selection of basalt as an additive are that it is a low-cost natural material with a high thermal stability and it improves the mechanical properties of some polymers. For example, Niaki *et al.*¹⁵ achieved the mechanical properties of epoxy resin with a basalt aggregate additive of up to 25%. On the other hand, Szabó *et al.*¹⁶ obtained better mechanical performances in PP-polyamide blends by doping them with short basalt fibers.

EXPERIMENTAL

Materials

PP [melting temperature (T_m) = 165 °C, density = 0.905 g/cm³, molecular weight = 42.08 g/mol] was obtained from Petkim Industry (Turkey). Volcanic rocks (VRs), collected from Van City, Turkey, were used as an additive material for PP.

The chemical analysis of the VR powder was performed via X-Ray Fluorescence (XRF) measurements on a model X-123SDD instrument from Amptek, and the operating conditions were set at 30 kV and 100 μ A. The chemical composition of the VR powder is given in Figure 1.

As shown in Figure 1, the VR powder contained 41.69% SiO₂ and 6.98% Na₂O plus K₂O. Because the VR powder contained SiO₂ at concentrations between 41–45% and had an Na₂O plus K₂O content of less than 7% w/w, according to the total alkali silica classification of VRs,¹⁷ the VR powder was considered tephrite basanite.

Preparation of the PP-Basalt Thick Films

The PP and basalt powders were mixed with different basalt concentrations from 0.5 to 10.0%. To obtain a homogeneous composition, these powder mixtures were ground with an IKA A11 basic analytical mill at a rotational speed of 10,000 rpm for 15 min. After the grinding process, the PP-basalt composites were prepared by a hot-press process. The pressing procedure involved a preheating step at 438 K for 20 min; this was followed by compression for 10 min at the same temperature under a pressure of 15 MPa. Finally, a homogeneous film was obtained for each melting mixture. At the end of the hot-press process, the thick films were cooled in a flow of cold water. Although the thicknesses of the samples, measured with a Mitutoyo micrometer, varied between 71 and 100 μ m, the diameter of all of the samples was 24 mm.

γ -Ray Irradiation Process of the Samples

The PP and PP-basalt thick films were irradiated with a γ irradiator (Nordion JS 9600 model, Canada) with an 861.368 kCi (⁶⁰Co) source. Irradiation was carried out at room temperature (23 °C) in air at the GAMMA-PAK A.S. plant (Çerkezköy, Tekirdağ, Turkey). The irradiation doses were measured with Harwell Amber 3042 and Red Acrylic Perspex 4034 dosimeters. The average dose rate was 2.9 kGy per unit hour.

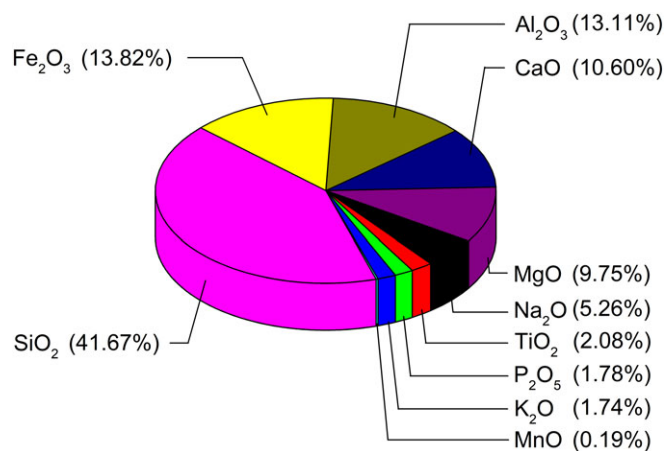


Figure 1. Chemical composition of the basalt powder. [Colour figure can be viewed at wileyonlinelibrary.com]

Scanning Electron Microscopy (SEM) Micrographs of the Samples

The surface morphologies of the pure PP and basalt and some of the PP–basalt composite films for different γ -ray doses were viewed with a Zeiss EVO LS 10 model scanning electron microscope.

FTIR Spectroscopy of the Samples

FTIR spectra of the samples were obtained with a PerkinElmer Spectrum 400 One FTIR spectrometer in the transmittance mode in the wave-number interval of 4000–400 cm^{-1} with a resolution of 2 cm^{-1} after four scans. The FTIR spectra of the γ -irradiated samples were obtained after 15 days in air from the irradiation process.

Differential Scanning Calorimetry (DSC) Characterization of the Samples

To reveal how the thermal properties of the samples were changed by the irradiation process of γ photons, DSC analysis was used. The thermal analysis was performed with a Shimadzu DTG 60H-DSC 60. Samples with masses that varied between 0.620 and 1.824 mg were heated from 26 to 200 $^{\circ}\text{C}$ at a rate of 10 $^{\circ}\text{C}/\text{min}$. For each sample, DSC analysis was repeated three times. The melting and crystallization data were also determined from the second scan.

Characterization of the Mechanical Properties of the Thick Films

The mechanical properties of the thick films were evaluated with a Lloyd Instruments LF Plus single-column universal materials testing machine with a crosshead speed of 50 mm/min at 23 ± 3 $^{\circ}\text{C}$. Tensile tests were also performed according to ASTM D 882. The dimensions of the tensile test specimen were as follows: gauge length = 4 mm, thickness = 71–100 μm , cross-sectional area = $4 \times (0.071\text{--}0.100)$ mm^2 . Test methods from ASTM D 882 were used to test specimens in the form of thin sheeting with a thickness of less than 1.0 mm (0.04 in.). The mechanical measurements were repeated three times with three samples cut from different parts of the same thick film. We determined each mechanical parameter value by taking an arithmetic mean.

Characterization of the Dielectric Properties of the Thick Films

Impedance measurements were performed with an HP 4194A impedance analyzer at frequencies between 100 Hz and 15 MHz with a high accuracy of 0.17% at room temperature. Gold electrodes with a diameter of 2 cm were used as a parallel-plate capacitor. As the dielectric materials, the thick films were placed between the gold electrodes. The experimental results were transferred to a computer with a GPIB data cable and simultaneously recorded by the computer. The real and imaginary components of the complex dielectric function (ϵ' and ϵ'' , respectively) were calculated with the capacitance (C), conductance (G), and loss tangent ($\tan \delta$) values. The relations between these physical quantities are given in the following equations:

$$\epsilon' = \frac{Cd}{A\epsilon_0} \quad (1)$$

$$\epsilon'' = \frac{Gd}{A\epsilon_0} \quad (2)$$

$$\epsilon'' = \epsilon' \tan \delta \quad (3)$$

where ϵ_0 is the elastic limit value of the strain for each sample. The d and A parameters are the thickness of the thick films and the active electrode area, respectively. Although ϵ' defines the charge-storage ability of the dielectric material, ϵ'' describes the dielectric loss.

RESULTS AND DISCUSSION

SEM Analysis of the Samples

The SEM micrographs for the pure PP and basalt and some of the PP–basalt composite films are shown in Figure 2.

As shown in Figure 2(a), the basalts were viewed as irregularly shaped rocks. The average size of the basalt rocks varied between 1 and 7 μm . On the other hand, the pure PP had an almost smooth surface. When 0.5% basalt was added to the pure PP, no considerable change in the surface morphology was observed [see Figure 2(c)]. When the basalt additive percentage was increased in the PP matrix, an increasing number of swellings was observed [see Figure 2(f,i)]. Additionally, as shown in Figure 2(i), the basalt additive was distributed homogeneously in the PP.

Although no significant change was observed in the morphology of the composites irradiated with a low dose of γ rays (3 kGy and 12k Gy), minor degradation was observed for the composites irradiated by a 25 kGy dose of γ rays. Similar behavior has already been reported by other studies.^{18–20}

Ultimately, we deduced that the high basalt additive and γ -irradiation dose disrupted the surface morphology of the PP. This deformation may have led to worse mechanical properties. This prediction was verified, as discussed in the mechanical analysis section.

FTIR Spectrum Analysis of the Samples

The FTIR spectra of the neat PP with different irradiation doses are shown in Figure 3(a).

In the spectrum of the pristine PP, related characteristic bands were observed as follows:^{21–25}

1. The broad band around 3300–3450 cm^{-1} was the characteristic band of the hydroxyl groups (O–H stretching).
2. The bands at 2959 and 2870 cm^{-1} corresponded to the asymmetric stretching oscillations of the CH_2 and CH_3 groups and the symmetric stretching oscillations of the CH_3 groups.
3. The bands at 1460 cm^{-1} were related to the asymmetric bending deformation oscillations of the CH_3 groups.
4. The bands at 1377 cm^{-1} were specific for the symmetric bending oscillations of CH_3 groups and CH_2 wagging vibrations.
5. The band in the vicinity of 1168 cm^{-1} corresponded to C–C chain stretching, CH bending, and CH_3 rocking vibrations.
6. The band at 998 cm^{-1} was related to CH_3 rocking, CH_2 wagging, and CH bending oscillations.

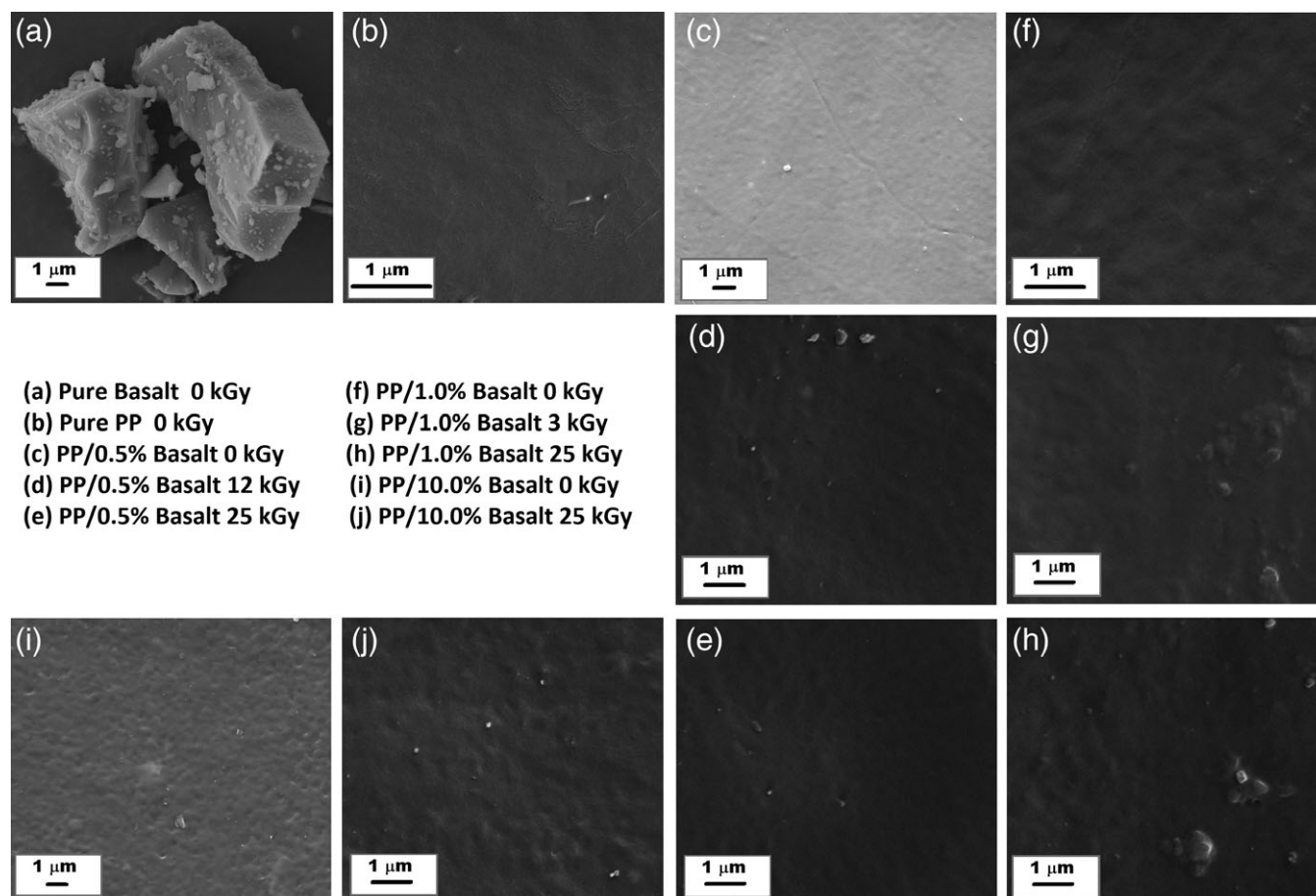


Figure 2. Micrographs of the pure PP and basalt along with some of the PP–basalt composite films for different γ -ray doses.

- The band at 973 cm^{-1} was assigned to C–C chain stretching and CH_3 rocking oscillations.
- The band at 841 and 810 cm^{-1} was related to CH_2 rocking and C– CH_3 stretching oscillations.

According to the characteristic bands observed near 1168 , 998 , and 973 cm^{-1} in the spectrum of the pristine PP, the polymer was considered as isotactic. The methyl group was also located on one side of the plane of the carbon atom chain, and the structure of isotactic PP is shown in Figure 4.

In general, the presence of the same main bands in the γ -irradiated PP indicated that the intrinsic nature of PP was not destroyed by the γ irradiation [Figure 3(a)]. However, the increase in the intensity of the bands in the $3500\text{--}3200\text{ cm}^{-1}$ interval revealed the increasing number of hydroxyl groups (O–H stretching) in the irradiated PP [Figure 3(a)].²⁶ Additionally, as shown in Figure 3(a), a slight change in the transmittance percentage of all of the bands in the whole spectrum of PP was observed with increasing γ exposure. This effect implied the occurrence of chain scission and crosslinking due to the γ rays.⁸ Furthermore, increasing irradiation doses led to the appearance of a new band at 760 cm^{-1} [Figure 3(a)]. This band was also associated with the segments of a new disordered region in the polymer, within which were localized vibrations characteristic of the conformation of the segments.²⁷

In Figure 3(b), unirradiated PP, basalt, and some of the PP–basalt films are shown together to emphasize the influence of the basalt additive on the FTIR spectrum of PP. Characteristic basalt bands were observed between 600 and 1200 cm^{-1} :

- The wide band observed around 1000 cm^{-1} for basalt was attributed to the asymmetric stretching of Si–O, which generally occurs between 900 and 1200 cm^{-1} .²⁸
- The band at 700 cm^{-1} also corresponded to the Fe–O bonds.²⁹
- While the bands at 595 and 656 correspond to Al–O stretching mode, the band at 715 cm^{-1} was assigned to the symmetric bending of Al–O–H.³⁰

When the FTIR spectra of the neat PP and 0.5 and 10% basalt-doped PP were compared, we determined that the characteristic transmittance bands of PP, observed between 900 and 1200 cm^{-1} , were extended because of the basalt additive [see Figure 3(b)]. The widening of the band of PP may have also been due to the high SiO_2 content of the basalt additive. Moreover, a new band was observed between 650 and 750 cm^{-1} because of the increasing basalt additive content. This new band was attributed to Al_2O_3 (715 cm^{-1}) and Fe_2O_3 (700 cm^{-1}), which were the other two main components of the basalt.²¹

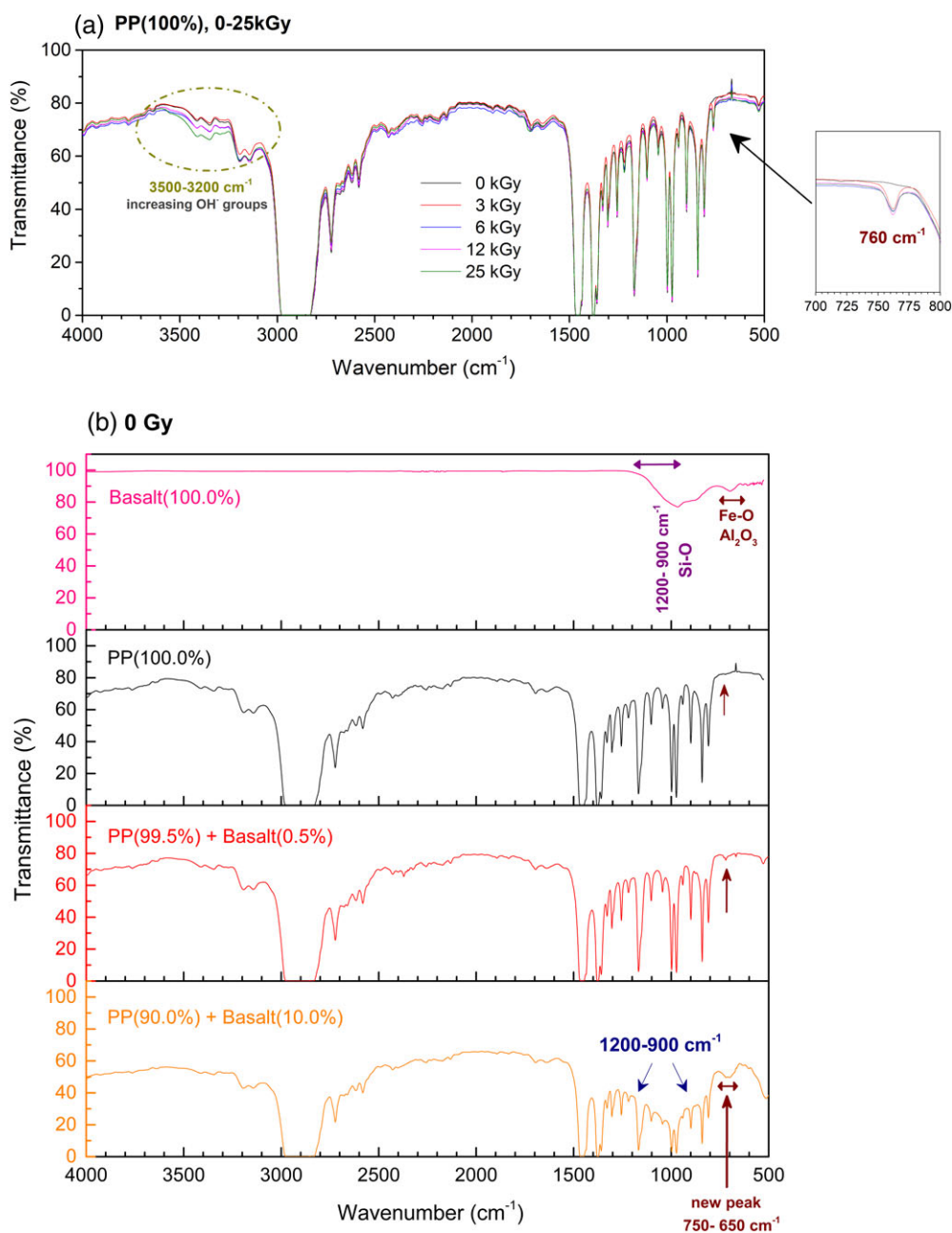


Figure 3. (a) Depiction of the FTIR spectra of PP at different γ -irradiation doses and (b) FTIR spectra of the pure basalt, pure PP, and some of the PP-basalt films at 0 kGy. [Colour figure can be viewed at wileyonlinelibrary.com]

To investigate the influence of the γ -irradiation process on the PP-basalt film, the FTIR spectra of the PP-10% basalt film are also shown in Figure 5(a). No additional band was observed in the FTIR spectrum of the γ -irradiated PP-10% basalt composite film. However, the bands observed between 3200 and 3500 cm^{-1} were extended with increasing γ dose. This may have indicated a possible increase in the formation of hydroxyl groups. The formation of hydroxyl groups due to γ irradiation in the FTIR spectrum of PP was already been reported by Sinha *et al.*²⁴ Additionally, the transmittance of the film decreased by 3 to 4% when it was exposed to 25 kGy γ irradiation.

As shown Figure 5(b), all of the PP-basalt films, including pure PP at 3 kGy, showed a change in the intensity of the characteristic bands between 1300 and 800 cm^{-1} . The decrease in the intensity of the related characteristic bands of the composite film were mostly attributed to the effect of the basalt additive. The

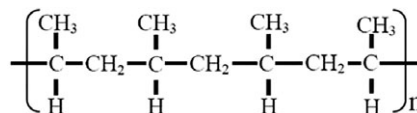


Figure 4. Structure of the isotactic PP.

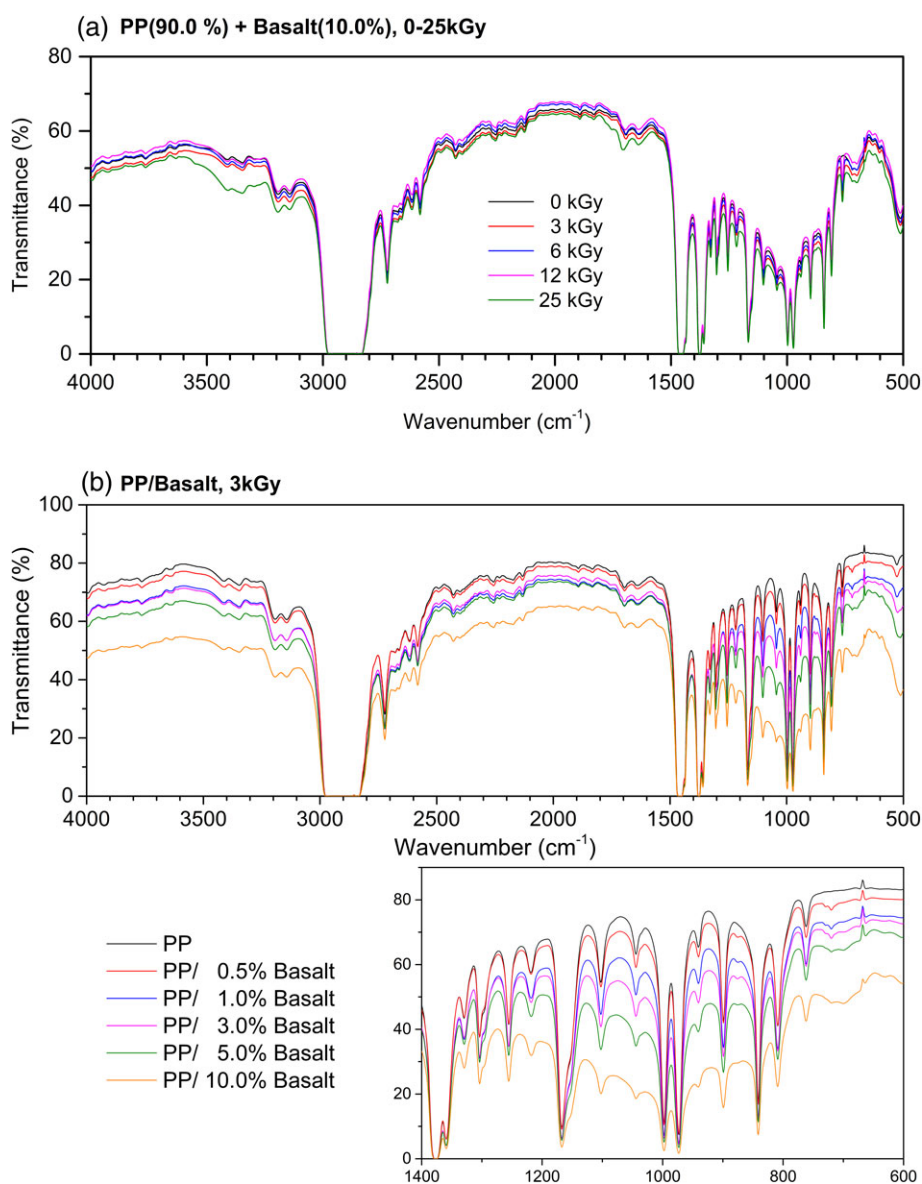


Figure 5. FTIR spectra of (a) the PP/10% basalt film at different γ -irradiation doses and (b) all PP–basalt films, including pure PP, at 3 kGy. [Colour figure can be viewed at wileyonlinelibrary.com]

influence of γ irradiation on the samples' structures was also investigated by DSC analysis.

DSC Analysis of the Samples

As is known, the γ -irradiation process may cause crosslinking and/or scission of the molecular chains of polymers or even degradation and destruction of the macromolecules. Degradation and destruction of the macromolecules may indicate the formation of the molecules with small chain lengths or changes in the number or nature of the double bonds within the polymer backbone.^{31–33} In the process of γ irradiation of polymers, crosslinking and chain scission (chain shortening) can occur at the same time. The chain-scission process results in the breakdown of macromolecular chains and also an increase in T_m because of the tighter packing and

rearrangement of shortened polymer chains.³³ The crosslinking process also causes a progressive reduction in the crystallinity. Additionally, an increase in the crosslinking may cause a decrease in the T_m of polymers.³⁴ From this point of view, the influence of γ irradiation on the thermal properties and structure of the polymeric materials were evaluated in the context of DSC heating and cooling curves. The related thermal graphics for the neat PP and 0.5% basalt-added PP samples are given in Figure 6.

According to Figure 6, some characteristic temperatures, such as T_m and the crystallization temperature (T_c), were determined and are also listed in Table I. Additionally, the degree of crystallinity (X_c) was calculated by eq. (4) and is given in Table I:

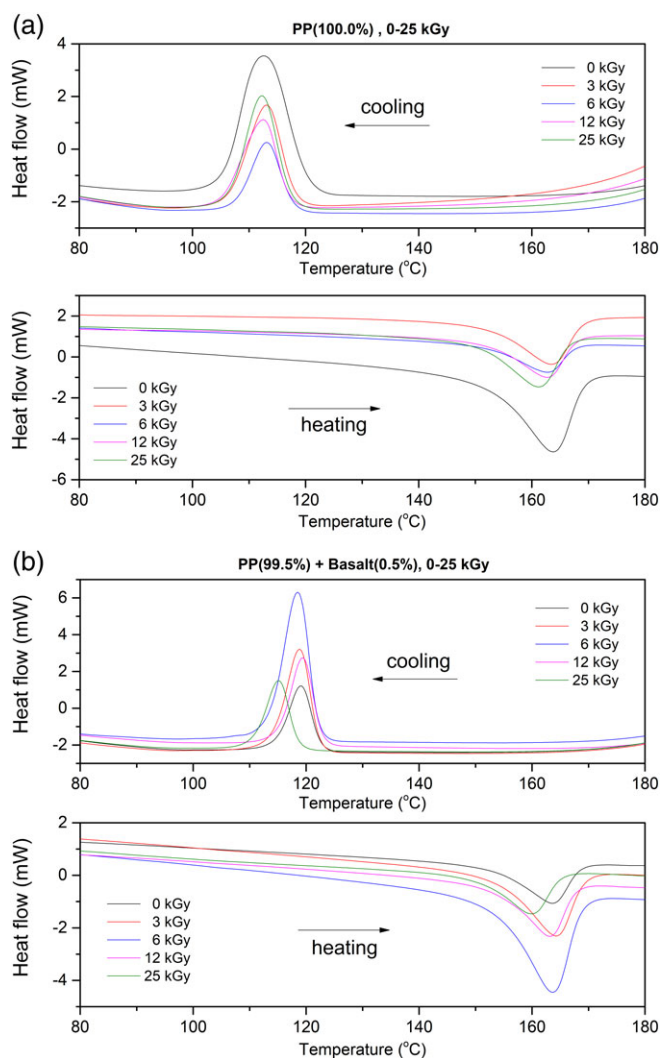


Figure 6. DSC heating and cooling curves of the (a) PP (100%) and (b) PP (99.5%)–basalt (0.5%) samples for the γ -irradiation doses of 0, 3, 6, 12, and 25 kGy. [Colour figure can be viewed at wileyonlinelibrary.com]

$$X_c = \left(\frac{\Delta H_m}{\Delta H_{100\%}} \right) \times 100 \quad (4)$$

where ΔH_m and $\Delta H_{100\%}$ are the heats of melting of the sample and the 100% crystalline PP. The $\Delta H_{100\%}$ for the neat PP was taken as 207 J/g.³⁵

As shown in Figure 6(a), neat PP had one T_m and T_c observed during the heating and cooling process, respectively. The T_m of neat PP was determined to be 163.7 °C; this was in good agreement with the catalog value of 165 °C³⁶ (see Table I). As observed in Figure 6(b), the addition of 0.5% basalt changed T_m and T_c for the γ -irradiated samples. However, no significant change was observed for the T_m of PP at 0 kGy because of basalt doping. Moreover, no additional T_m or T_c values were observed for the composite. This was due to the high T_m of basalt. As is known, because basalt is an igneous rock that forms through the crystallization of magma, it has a T_m in the vicinity of 1200 °C.³⁷

As shown in Table I, the effect of γ irradiation manifested itself as a change in both T_m and T_c . Additionally, we observed that 12 and 25 kGy γ -irradiation doses decreased T_m . In particular, the 25 kGy dose reduced T_m by approximately 1.47 and 2.26% for the pristine PP and 0.5% basalt-added PP, respectively. In this respect, we deduced that high γ -irradiation doses caused more degradation in the composite because of the basalt additive. This degradation could be explained by the possible occurrence of the reduction of the molecular weight of the polymer because of high-energy irradiation; this resulted in decreased T_m s. Additionally, lower T_m s indicated reduced crystallinities because of increasing crosslinking degradation in the materials after γ irradiation. On the other hand, we determined that after 3 kGy γ irradiation, the 0.5% basalt-added PP samples had higher T_m s relative to the pristine ones. From this point of view, we concluded that the low γ -ray photons caused a chain-scission process in the basalt-added samples. Our interpretation was also consistent with the result suggested by Black and Lyons.³⁸ They showed that the chain scission was disproportionately higher at low doses of high-energy radiation in PP.

Mechanical Analysis of the Samples

The variation of the mechanical properties of neat PP with basalt doping was investigated in our previous study.²¹ According to these results, the highest tensile strength, percentage

Table I. Some Characteristic Temperatures and Parameters for the Neat PP and 0.5% Basalt-Doped PP Composites for Different γ -Irradiation Doses

Sample	Irradiation dose (kGy)	T_i (°C)	T_f (°C)	T_c (°C)	T_m (°C)	ΔH_m (J/g)	X_c (%)
PP (100%)	0	120.4	105.4	112.6	163.7	104.6	50.5
	3	118.5	106.4	113.2	163.3	99.5	48.0
	6	118.2	107.4	113.3	162.8	91.0	43.9
	12	117.2	104.9	112.5	162.7	97.2	46.9
	25	117.8	106.5	112.4	161.3	88.9	42.9
PP (99.5%)–basalt (%0.5)	0	122.7	114.6	119.2	163.4	99.2	47.9
	3	122.7	113.9	118.9	164.3	75.1	36.3
	6	122.4	113.6	118.5	163.5	90.42	43.7
	12	123.2	115.2	119.5	163.2	86.94	42.0
	25	118.9	110.5	115.1	159.7	92.4	44.6

T_f , final temperature of the melting peak; T_i , initial temperature of the melting peak.

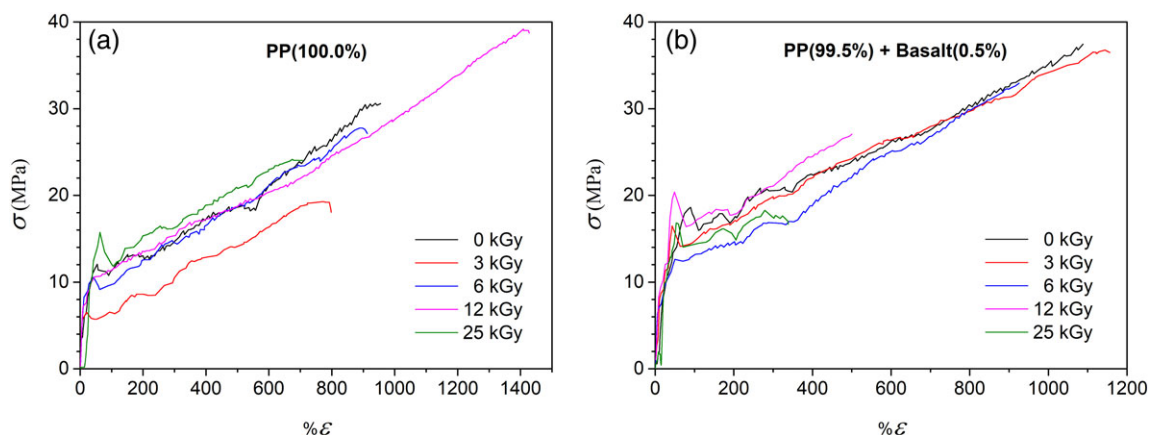


Figure 7. Stress (σ)–strain (ϵ) curves under 0–25 kGy of γ -ray irradiation for the (a) neat PP and (b) PP (99.5%)–basalt (0.5%). [Colour figure can be viewed at wileyonlinelibrary.com]

strain, and energy at break values were obtained for the 0.5% basalt additive. In this study, the influence of γ irradiation on the mechanical properties of the neat PP and PP–basalt composites were examined. The mechanical properties of the samples, such as the tensile strength, Young's modulus, percentage strain, and energy at break, were determined with stress–strain curves.

The effects of high-dose γ irradiation on the stress–strain curves for some of the samples are shown in Figure 7(a,b). Similar stress–strain curves were observed for the other samples.

As shown in Figure 7, the stress–strain curves of the neat PP (100%) and PP (100.0%)–basalt (0.5%) samples had two deformation regions called the elastic (i.e., linear) and plastic deformation regions and a breaking point. The influences of γ ray

irradiation and basalt addition on the elastic and plastic deformation regions of the samples are also given in detail in Figures 8 and 9, respectively.

As shown in Figure 8, the maximum elasticity was obtained for the unirradiated 0.5% basalt-added composite. On the other hand, among all of the composites, the 6 kGy γ -irradiated PP (99.0%)–basalt (1.0%) sample exhibited the highest elasticity properties. From the plastic deformation point of view, where the neat PP showed the highest plastic properties for the 12 kGy γ irradiation, only the 3 kGy γ -irradiated 0.5 and 1.0% basalt-doped PP composites displayed relatively high plastic properties. All of the mechanical parameters for all samples under the influence of different γ -irradiation doses are also summarized in Table II. As shown in Table II, the 0.5% basalt-doped PP sample had the highest energy at break value after 3 kGy γ irradiation. The highest energy at break value observed for 3 kGy γ irradiation; this

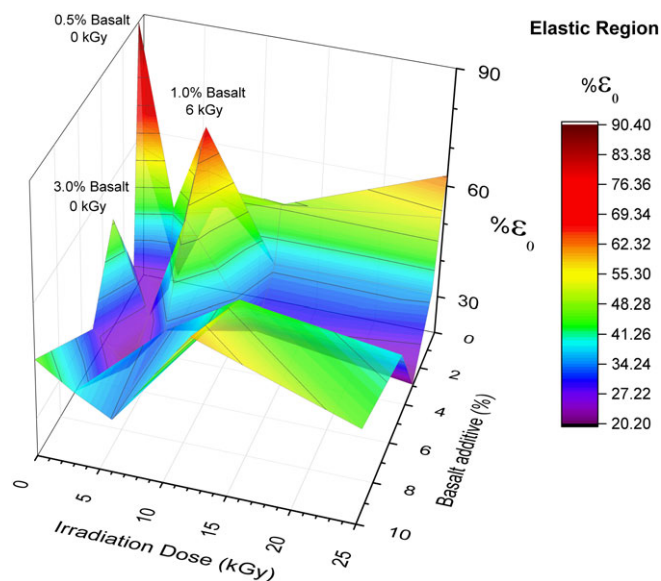


Figure 8. Influence of both the γ -ray irradiation and the basalt additive on the elastic region of the samples. (The strain related to the elastic deformation is ϵ_0 .) [Colour figure can be viewed at wileyonlinelibrary.com]

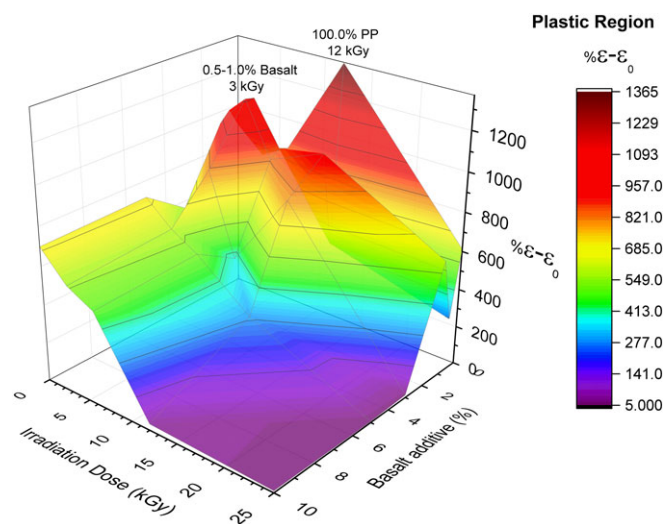


Figure 9. Influence of both the γ -ray irradiation and the basalt additive on the plastic region of the samples. (The strain related to the plastic deformation is $\epsilon - \epsilon_0$.) [Colour figure can be viewed at wileyonlinelibrary.com]

Table II. Mean and Standard Deviation Values of the Mechanical Parameters for All Samples Irradiated by γ Rays with Doses of 0–25 kGy

Sample	Irradiation dose (kGy)	Tensile strength (MPa)	Young's modulus (MPa)	Strain at break (%)	Energy to break (mJ)
PP (100.0%)	0	30.62 ± 1.53	120.68 ± 9.02	976.06 ± 58.56	38.28 ± 2.32
PP (99.5%)–basalt (0.5%)		37.67 ± 2.26	71.75 ± 4.71	1103.85 ± 72.37	51.2 ± 4.34
PP (99.0%)–basalt (1.0%)		27.04 ± 1.08	75.35 ± 5.05	986.87 ± 63.17	30.01 ± 2.71
PP (97.0%)–basalt (3.0%)		18.55 ± 1.57	89.38 ± 7.59	635.15 ± 53.97	16.73 ± 1.47
PP (95.0%)–basalt (5.0%)		17.41 ± 0.93	92.09 ± 7.36	755.91 ± 51.05	14.43 ± 1.15
PP (90.0%)–basalt (10.0%)		22.05 ± 1.32	124.07 ± 11.44	770.65 ± 34.01	24.45 ± 1.79
PP (100.0%)	3	19.28 ± 1.06	110.74 ± 6.09	796.88 ± 43.83	14.19 ± 0.78
PP (99.5%)–basalt (0.5%)		36.76 ± 1.73	139.35 ± 6.55	1237.84 ± 58.18	59.52 ± 2.80
PP (99.0%)–basalt (1.0%)		25.72 ± 0.90	74.35 ± 2.60	1137.73 ± 39.82	32.59 ± 1.14
PP (97.0%)–basalt (3.0%)		22.10 ± 1.33	114.94 ± 6.89	847.36 ± 50.74	24.52 ± 1.47
PP (95.0%)–basalt (5.0%)		20.10 ± 1.06	110.38 ± 5.85	643.88 ± 34.13	16.72 ± 0.89
PP (90.0%)–basalt (10.0%)		22.03 ± 1.06	162.42 ± 7.79	604.24 ± 29.01	20.31 ± 0.97
PP (100.0%)	6	27.76 ± 1.08	106.92 ± 4.17	913.79 ± 35.64	32.33 ± 1.16
PP (99.5%)–basalt (0.5%)		32.94 ± 1.45	158.27 ± 6.96	925.75 ± 40.73	35.33 ± 1.55
PP (99.0%)–basalt (1.0%)		31.42 ± 1.94	112.11 ± 6.95	904.61 ± 56.08	36.78 ± 2.28
PP (97.0%)–basalt (3.0%)		23.02 ± 0.65	133.46 ± 3.74	464.66 ± 13.01	15.59 ± 0.44
PP (95.0%)–basalt (5.0%)		20.74 ± 0.95	218.94 ± 10.07	561.87 ± 25.85	19.04 ± 0.88
PP (90.0%)–basalt (10.0%)		20.46 ± 1.13	162.22 ± 8.92	535.05 ± 29.43	17.35 ± 0.95
PP (100.0%)	12	39.18 ± 2.39	99.82 ± 6.09	1428.44 ± 87.13	68.16 ± 4.16
PP (99.5%)–basalt (0.5%)		27.13 ± 1.19	114.29 ± 5.03	554.83 ± 24.41	19.86 ± 0.87
PP (99.0%)–basalt (1.0%)		29.65 ± 1.51	136.03 ± 6.94	998.55 ± 50.93	42.06 ± 2.15
PP (97.0%)–basalt (3.0%)		24.35 ± 0.91	133.04 ± 4.92	839.57 ± 31.06	26.69 ± 0.98
PP (95.0%)–basalt (5.0%)		20.19 ± 0.97	200.76 ± 9.64	378.43 ± 18.16	11.53 ± 0.5
PP (90.0%)–basalt (10.0%)		19.78 ± 1.23	207.06 ± 12.84	103.06 ± 6.39	1.88 ± 0.11
PP (100.0%)	25	24.16 ± 1.39	89.19 ± 5.08	714.79 ± 40.698	23.22 ± 1.32
PP (99.5%)–basalt (0.5%)		18.27 ± 0.89	172.56 ± 8.45	335.31 ± 16.43	8.78 ± 0.43
PP (99.0%)–basalt (1.0%)		14.68 ± 0.57	86.72 ± 3.38	675.39 ± 26.34	13.98 ± 0.55
PP (97.0%)–basalt (3.0%)		13.39 ± 0.84	133.15 ± 8.39	35.14 ± 2.22	0.65 ± 0.04
PP (95.0%)–basalt (5.0%)		18.40 ± 1.19	99.92 ± 6.49	45.70 ± 2.97	0.75 ± 0.04
PP (90.0%)–basalt (10.0%)		16.65 ± 0.92	110.50 ± 6.08	59.55 ± 3.27	1.34 ± 0.07

corresponded to the highest mechanical strength against breakage. Because the high energy at break value corresponded to the material with high resistance to break, this behavior was an indicator of reduced crystallinity due to the 3 kGy γ irradiation. This prediction was also confirmed by the observation of the lowest X_c of 36.3 for the 0.5% basalt-doped PP composite (see Table I). This behavior was also explained by both the tight packing and rearrangement of the shortened polymer chains after 3 kGy γ irradiation. This result was also in a good agreement with the prediction of the occurrence of chain scission for the 0.5% basalt-doped PP composite from DSC analysis given earlier. Moreover, the lowest energy at break value for the 0.5% basalt-doped sample was observed for 25 kGy γ irradiation. As is known, the lowest energy at break value indicates that the sample can be broken with a lower energy requirement. The lowest energy at break value was possible with the occurrence of increased

crystallinity in the material relative to the 3 kGy γ -irradiated sample.

According to Table II, the variations in the tensile strength with the basalt additive for different γ -irradiation doses, including 0 Gy, are shown in Figure 10.

As is clearly shown in Figure 10, although the application of 12 kGy γ irradiation was very effective for achieving the highest tensile strength for the neat PP, the highest dose of γ irradiation decreased the tensile strength of the PP composites that contained up to 3% basalt additive. In light of the mechanical analysis, we deduced that increasing the γ -irradiation dose caused degradation (i.e., crosslinking) for PP. In addition, the decrease in the tensile strength values for the basalt-doped samples could be interpreted as the formation of free radicals in the materials.

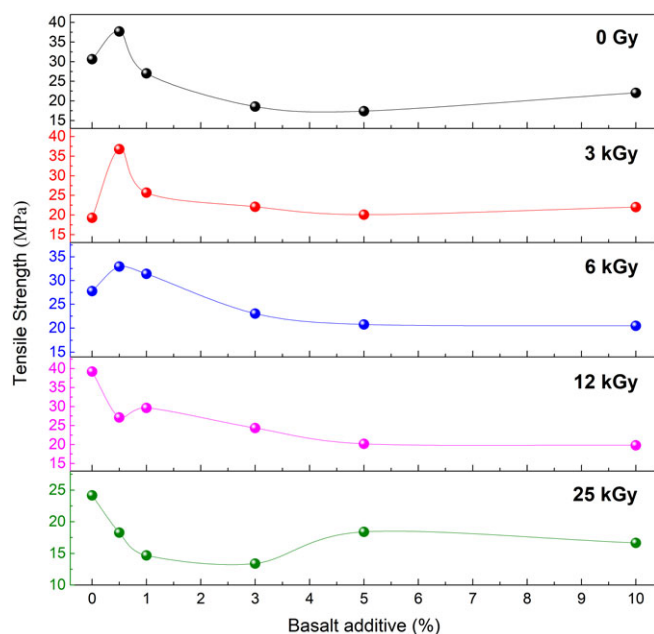


Figure 10. Variation of the tensile strength with the basalt additive concentration at doses of 0, 3, 6, 12, and 25 kGy. [Colour figure can be viewed at [wileyonlinelibrary.com](https://onlinelibrary.wiley.com/doi/10.1002/app.47414)]

Dielectric Analysis of the Thick Films

The effect of basalt doping on the dielectric properties of neat PP was investigated in our previous study, and the lowest ϵ' value was achieved for 0.5% basalt doping, whereas the dielectric loss remained the same.²¹ In this study, the effects of γ -ray irradiation on the dielectric properties of the neat PP and PP–basalt composites were also investigated. The variations of ϵ' and ϵ'' for the neat PP and PP composites with basalt additive under the influence of various γ -ray doses are given in Figures 11 and 12, respectively.

According to Figure 11, all of the samples had a nearly frequency-independent dielectric constant in a wide frequency interval between 100 Hz and 2 MHz. Then, they exhibited a strong dispersion between frequencies of 2 MHz and 15 MHz. The almost frequency-independent behavior of ϵ' up to 2 MHz indicated the insulating and less polar nature of the samples. On the other hand, the strong dispersion above 2 MHz may have been an indicator of space-charge polarization in the samples.

As shown in Figure 11, neither the basalt additive nor the γ -irradiation process changed the frequency-dependence characteristics of ϵ' . On the other hand, 3 kGy γ -ray exposure remarkably decreased the ϵ' value of the neat PP. Additionally, ϵ' decreased with basalt addition but increased with the application of γ irradiation [see Figure 11(a–f)]. Moreover, although the ϵ' value increased for the neat PP after 25 kGy γ irradiation, the composites' ϵ' values increased hierarchically with increasing γ -irradiation doses except for in the 1.0% basalt-doped composite. From this point of view, we deduced that radiation-induced crosslinking effect at higher γ doses had a more crucial role on dielectric properties of PP than the chemical crosslinking produced by basalt doping. A similar result was observed in the dielectric results of electron-beam-irradiated PP by Pawde and

Parab.¹¹ Moreover, Raghu *et al.*⁸ pointed out an increase in the dielectric permittivity with increasing irradiation doses for polymers.

The dielectric constants of all of the samples were also determined by the linear extrapolation of the ϵ' versus frequency curves. When the 0 kGy and 25 kGy γ -ray-irradiated samples' dielectric constant were compared, an enhancing effect on the dielectric constant due to high-dose γ rays was revealed (see Table III). This behavior of ϵ' with the application of γ irradiation could be explained as the occurrence of some defect sites in the composites, which resulted in crosslinking. As is known, the irradiation of polymers with ionizing radiation, such as X-rays or γ rays, may cause reactive intermediate states or free radicals in the material; this results in the molecular crosslinking of chains, and destruction and degradation of the macromolecules.^{39,40} Additionally, free radicals formed by irradiation could have improved the crosslinking between the PP and basalt molecules.⁴ The occurrence of crosslinking after 25 kGy of irradiation was also predicted from the DSC results given earlier.

The investigation of the influence of γ -ray irradiation on ϵ'' of the samples revealed that γ irradiation doses of 3 and 6 kGy considerably decreased the dielectric loss for the 1.0 and 5.0% basalt-doped composites at high frequencies [see Figure 12(a–f)]. Moreover, although neat PP displayed sharp molecular vibration peaks in the ϵ'' versus frequency spectra for all γ -ray irradiation doses, the 3.0, 5.0, and 10.0% basalt-added composites exhibited relatively broad molecular rotation peaks, especially for the 3 and 6 kGy γ -ray irradiation doses. In this context, we determined that the 3 and 6 kGy γ irradiation may have caused chain scission on these composite materials. Furthermore, we determined that when the dielectric loss was lowered for the 1.0 and 5.0% basalt-doped composites, their frequency-dependent dielectric constant values increased with the application of 3 and 6 kGy γ -ray irradiation. With this context, we concluded that because the γ -ray irradiation at 3 and 6 kGy doses enhanced the charge-storage ability and decreased the dielectric loss for the PP (99%)–basalt (1.0%) and PP (95.0%)–basalt (5.0%) composites, these materials may be used in capacitor applications.

Also, the 3 kGy γ -ray irradiation reduced the values of both ϵ' and ϵ'' of the neat PP; this makes the neat PP a preferred material for microelectronic applications that require a low dielectric constant and loss.

The alternating-current conductivity (σ_{ac}) of the samples prepared was calculated with eq. (5):

$$\alpha_{ac}(\omega) = \omega \epsilon_0 \epsilon'' \quad (5)$$

where ω is the angular frequency. The ω dependences of the samples are shown in Figure 13. As shown in Figure 13, σ_{ac} of the PP was almost unchanged with the basalt contribution; with exposure to 25 kGy radiation, the conductivity increased slightly.

CONCLUSIONS

In this article, we have discussed the high-dose γ -ray irradiation responses of PP–basalt thick films in terms of the tensile

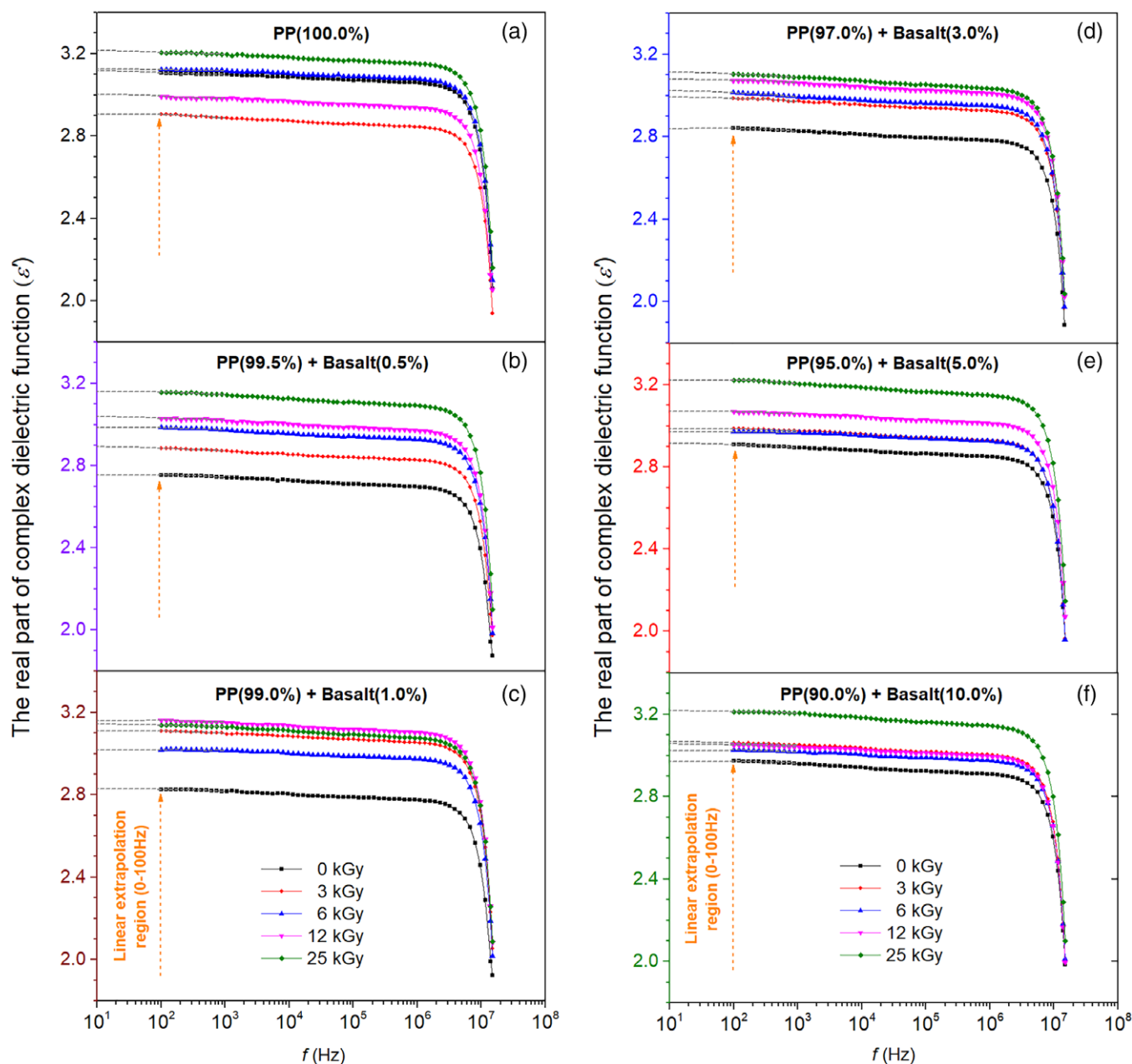


Figure 11. Frequency (f) dependence of ϵ' of the neat PP and PP–basalt samples under different doses of γ irradiation. [Colour figure can be viewed at [wileyonlinelibrary.com](https://onlinelibrary.wiley.com/doi/10.1002/app.47414)]

and dielectric properties. The influence of γ irradiation manifested itself as an occurrence of increasing frequency-independent dielectric constant values for all of the composites. This effect was associated with the occurrence of some defect sites in the composites, which resulted in crosslinking. The polymer degradation due to γ irradiation was also marked on the FTIR spectra of the irradiated samples by a new peak at 760 cm^{-1} . Moreover, the decrease in hydroxyl (O–H) groups due to the γ -irradiation process was explained by the occurrence of polymer degradation in the neat PP. Furthermore, the DSC analysis of the neat PP and PP–basalt composite revealed radiation-induced chain scission and

crosslinking effects in the samples; this depended on the radiation dose.

The mechanical properties of the samples, including the Young's modulus, tensile strength, percentage strain at break, and energy at break, were determined by stress–strain curves. The highest tensile strength and energy break values were observed for the 12 kGy γ -ray-irradiated neat PP sample. On the other hand, although the maximum elasticity was obtained for the unirradiated 0.5% basalt-added composite, the 12 kGy γ -irradiated neat PP had the highest plastic properties. The complex dielectric spectra of the samples were investigated to determine possible technological applications of the samples. The complex dielectric

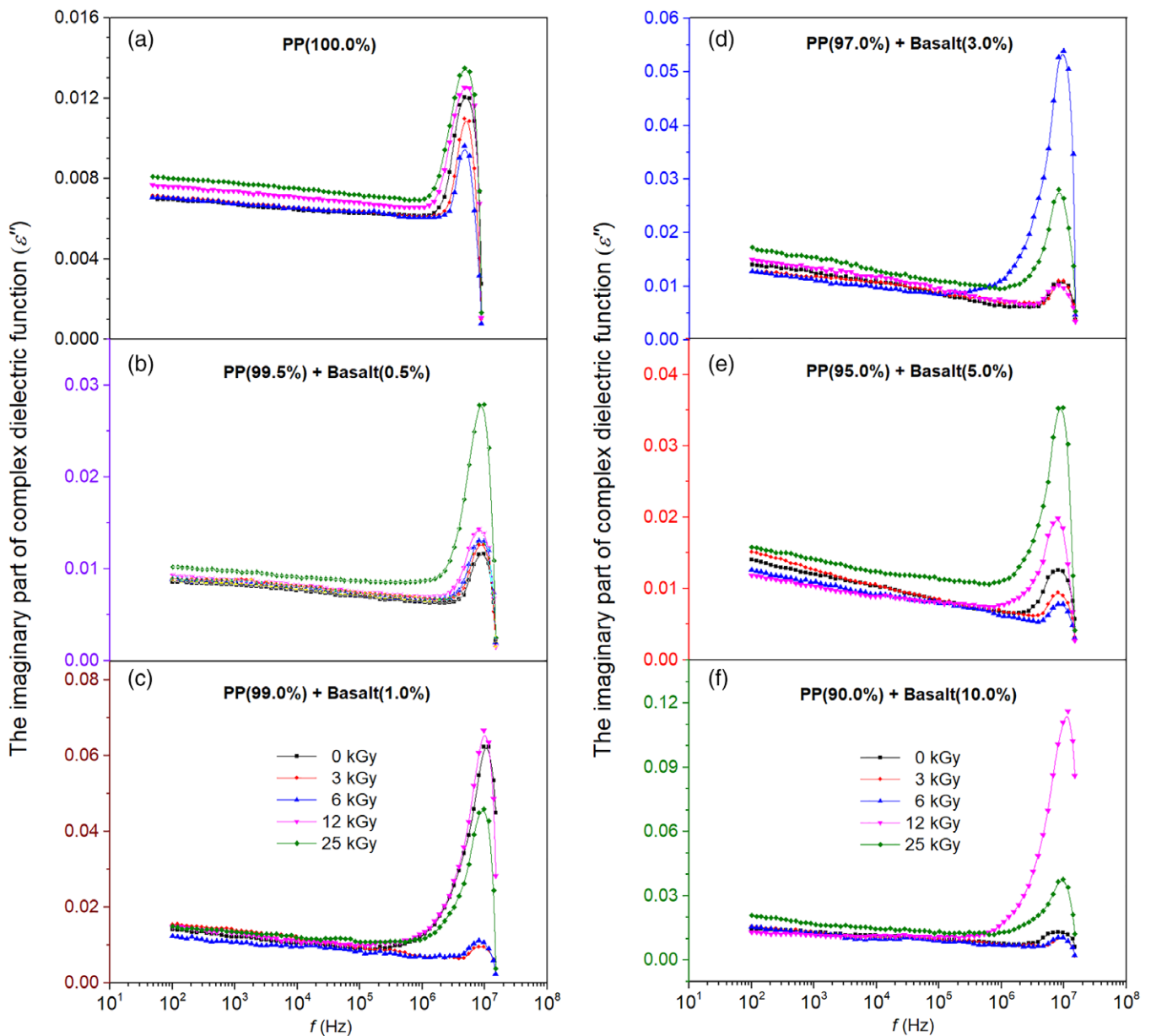


Figure 12. Frequency (f) dependence of ϵ'' of the neat PP and PP–basalt samples under different doses of γ irradiation. [Colour figure can be viewed at [wileyonlinelibrary.com](https://onlinelibrary.wiley.com/doi/10.1002/app.47414)]

Table III. Dielectric Constants of the Samples under Different γ -Ray Irradiation Conditions

Sample	Dielectric constant ^a				
	0 kGy	3 kGy	6 kGy	12 kGy	25 kGy
PP (100.0%)	3.12	2.90	3.13	3.00	3.21
PP (99.5%)–basalt (0.5%)	2.75	2.89	2.98	3.04	3.16
PP (99.0%)–basalt (1.0%)	2.83	3.11	3.02	3.16	3.14
PP (97.0%)–basalt (3.0%)	2.84	2.99	3.02	3.08	3.11
PP (95.0%)–basalt (5.0%)	2.91	2.99	2.97	3.07	3.22
PP (90.0%)–basalt (10.0%)	2.97	3.06	3.03	3.06	3.22

^a Nearly frequency-dependent value of ϵ' .

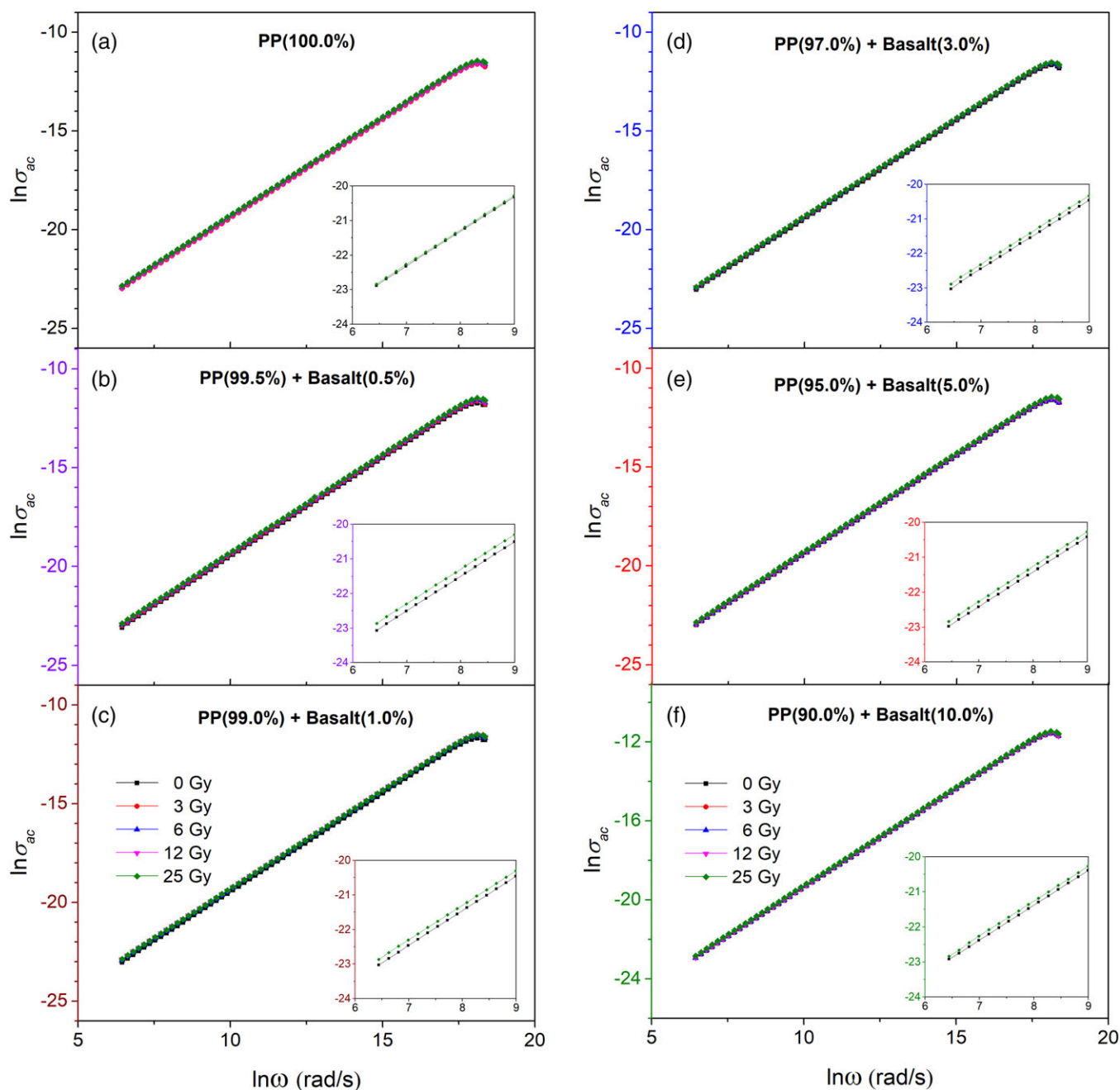


Figure 13. σ_{ac} versus ω for each sample with γ -radiation doses of 0, 3, 6, 12, and 25 kGy. [Colour figure can be viewed at wileyonlinelibrary.com]

spectra of the samples showed that the 3 kGy γ -irradiated neat PP may have potential for microelectronic packaging requiring low-dielectric-constant and dielectric-loss materials. In addition, the 3 and 6 kGy γ -ray-irradiated PP (99.0%)–basalt (1.0%) and PP (95.0%)–basalt (5.0%) composites may be used in capacitor applications because of their increased dielectric constants and reduced dielectric loss values.

ACKNOWLEDGMENTS

This work was supported by the Yildiz Technical University Scientific Research Projects Coordination Department under project 2015-01-01-GEP03.

REFERENCES

- García-Huete, N.; Laza, J.; Cuevas, J.; Vilas, J.; Bilbao, E.; León, L. *Radiat. Phys. Chem.* **2014**, *102*, 108.
- Moez, A. A.; Aly, S.; Elshaer, Y. *Spectrochim. Acta A.* **2012**, *93*, 203.
- Abiona, A. A.; Osinkolu, A. G. *Int. J. Phys. Sci.* **2010**, *5*, 960.
- Cota, S.; Vasconcelos, V. D.; Senne, M., Jr.; Carvalho, L.; Rezende, D.; Côrrea, R. *Braz. J. Chem. Eng.* **2007**, *24*, 259.
- Ghaffar, A. A.; Ali, H. *Bull. Mater. Sci.* **2016**, *39*, 1809.
- Nouh, S.; Abdel-Salam, M.; Radwan, Y. E.; Fouad, S. *Radiat. Effects Defects Solids.* **2011**, *166*, 178.

7. Fawzy, Y. H.; Ali, A. E.-H.; El-Maghraby, G. F.; Radwan, R. M. *World J. Condensed Matter Phys.* **2011**, *1*, 12.
8. Raghu, S.; Archana, K.; Sharanappa, C.; Ganesh, S.; Devendrappa, H. *J. Radiat. Res. Appl. Sci.* **2016**, *9*, 117.
9. Arranz-Andres, J.; Perez, E.; Cerrada, M. L. *IEEE Trans. Nanotechnol.* **2014**, *13*, 502.
10. Çakıroğlu, M. *Acta Phys. Polym. A.* **2016**, *129*, 705.
11. Pawde, S.; Parab, S. J. *Appl. Polym. Sci.* **2011**, *119*, 1220.
12. Keene, B.; Bourham, M.; Viswanath, V.; Avci, H.; Kotek, R. *J. Appl. Polym. Sci.* **2014**, 399917(1-10), 131 (<https://doi.org/10.1002/app.39917>).
13. Khan, M. A.; Khan, R. A.; Haydaruzzaman, A. H.; Khan, A. *J. Reinforced Plast. Compos.* **2009**, *28*, 1651.
14. Allahvaisi, S. Polypropylene; InTech: Rijeka, Croatia, **2012**.
15. Hassani Niaki, M.; Fereidoon, A.; Ghorbanzadeh Ahangari, M. *Struct. Concr.* **2018**, *19*, 366.
16. Szabó, J. S.; Kocsis, Z.; Czirány, T. *Periodica Polytech. Mech. Eng.* **2004**, *48*, 119.
17. Le Bas, M.; Le Maitre, R.; Woolley, A. *Miner. Pet.* **1992**, *46*, 1.
18. Gotsis, A.; Zeevenhoven, B.; Tsenoglou, C. *J. Rheol.* **2004**, *48*, 895.
19. Sawasaki, T.; Nojiri, A. *Int. J. Radiat. Appl. Instrum. Part C.* **1988**, *31*, 877.
20. Tian, J.; Yu, W.; Zhou, C. *Polymer.* **2006**, *47*, 7962.
21. Alkan, Ü.; Karabul, Y.; Bulgurcuoğlu, A. E.; Kılıç, M.; Özdemir, Z. G.; İçelli, O. *e-Polymers.* **2017**, *17*, 417.
22. Farrukh, M.; Simonescu, C. Advanced aspects of spectroscopy; InTech: Rijeka, Croatia **2012**.
23. Mathakari, N.; Bhoraskar, V.; Dhole, S. *Nucl. Instrum. Methods Phys. Res. Sect. B.* **2010**, *268*, 2750.
24. Sinha, D.; Swu, T.; Tripathy, S.; Mishra, R.; Dwivedi, K.; Fink, D. *Radiat. Effects Defects Solids.* **2003**, *158*, 531.
25. Türkçü, H. N. Ph.D. dissertation: "Investigation of the crystallinity and orientation of polypropylene with respect to temperature changes using FT-IR, WRD, and Raman techniques" Bilkent University, **2004**.
26. Perera, R.; Albano, C.; Gonzalez, J.; Silva, P.; Ichazo, M. *Polym. Degrad. Stab.* **2004**, *85*, 741.
27. Abdel-Hamid, H. *Solid-State Electron.* Vol. 49, **2005**. p. 1163.
28. Jaret, S. J.; Woerner, W. R.; Phillips, B. L.; Ehm, L.; Nekvasil, H.; Wright, S. P.; Glotch, T. D. *J. Geophys. Res. Planets.* **2015**, *120*, 570.
29. Sharma, R.; Lamba, S.; Annapoorni, S. *J. Phys. D. Solid-State Electronics.* **2005**, *49*, 1163.
30. Djebaili, K.; Mekhalif, Z.; Boumaza, A.; Djelloul, A. *J. Spectrosc.* **2015**, 2015, Article ID 868109. (<https://doi.org/10.1155/2015/868109>)
31. Lim, S.; Fane, A.; Fell, C. *J. Appl. Polym. Sci.* **1990**, *41*, 1609.
32. Shintani, H.; Kikuchi, H.; Nakamura, A. *Polym. Degrad. Stab.* **1991**, *32*, 17.
33. You, F.; Li, Y.; Zuo, Y.; Li, J. *Sci. World J.* **2013**, 2013, Article ID162384 (6 pages). (<https://doi.org/10.1155/2013/162384>).
34. Charlesby, A.; Ross, M. *Proc. R. Soc. Lond. A.* **1953**, *217*, 122.
35. Gee, D.; Melia, T. *Makromol. Chem. Macromol. Chem. Phys.* **1970**, *132*, 195.
36. Dikobe, D.; Luyt, A. *eXPRESS Polymers Letters* **2009**, *3*, 190.
37. Lutgens, F. K.; Tarbuck, E. J.; Tasa, D. G. *Essentials of Geology*; Pearson Higher Ed: New York, **2014**.
38. Black, R.; Lyons, B. *Proc. R. Soc. Lond. A.* **1959**, *253*, 322.
39. Bhattacharya, A. *Prog. Polym. Sci.* **2000**, *25*, 371.
40. Chmielewski, A. G.; Haji-Saeid, M.; Ahmed, S. *Nucl. Instrum. Methods Phys. Res. Sect. B.* **2005**, *236*, 44.